



Improved OAM-Based Radar Targets Detection Using Uniform Concentric Circular Arrays

Lin, M; Gao, Y; Liu, P; Liu, J

© 2016 Mingtuan Lin et al.

CC-BY

For additional information about this publication click this link.

<http://qmro.qmul.ac.uk/xmlui/handle/123456789/13013>

Information about this research object was correct at the time of download; we occasionally make corrections to records, please therefore check the published record when citing. For more information contact scholarlycommunications@qmul.ac.uk

Improved OAM-based Radar Targets Detection Using Uniform Concentric Circular Arrays

Mingtuan Lin, Yue Gao, Peiguo Liu, and Jibin Liu

Abstract—Without any relative moves or beam scanning, the novel Orbital-Angular-Momentum(OAM)-based radar targets detection technique using uniform concentric circular array (UCCA) shows the azimuthal estimation ability, providing new perspective for radar system design. However, the main estimation method Fast Fourier Transform (FFT) under this scheme suffers from low resolution. As a solution, this paper rebuilds the model and introduces the multiple signal classification (MUSIC) algorithm to improve the resolution for detecting targets within the main lobes. The spatial smoothing technique is proposed to tackle the coherent problem brought by the model. Simulation results demonstrate the super-resolution estimation capacity of the MUSIC algorithm for detecting targets within main lobes. In addition, the performance of the MUSIC algorithm to detect targets not illuminated by the main lobes is also evaluated. Despite the MUSIC algorithm loses the resolution advantage under this case, its estimation is more robust than the FFT approach. Overall, the proposed MUSIC method partly improves the performance of the OAM-based radar technique in terms of the high resolution ability, good robustness for detecting targets within and out of the main lobes.

Index Terms—OAM, MUSIC, spatial smoothing, super-resolution, radar target detection

I. INTRODUCTION

ORBITAL Angular Momentum (OAM) has been widely studied in the optic regime regarding imaging, microscopic particle and communication [1] [2]. However, OAM in radio frequency band had not been developed until 2007 when the feasibility of OAM generating in a low-frequency band was proved in [3]. Unlike the common planar wavefront in the far field, the twisted beam carrying OAM has a helical shape of wavefront known as a vortex. Benefiting from its peculiar properties such as the orthogonality of integer topological modes and larger degrees of freedom, OAM-based communication and radar techniques show a promising potential.

Previous works about radio OAM mainly focused on communication systems consisting of two subfields, namely performance analysis and design of antennas to generate twisted beams [4]–[9], and OAM multiplexing [10]–[13]. Radar based on this innovative concept had not attracted much attention until Guo et al. proposed OAM-based target detection model using the uniform circular array (UCA) in [14]. As depicted in Fig.1, instead of producing planar wave in a particular

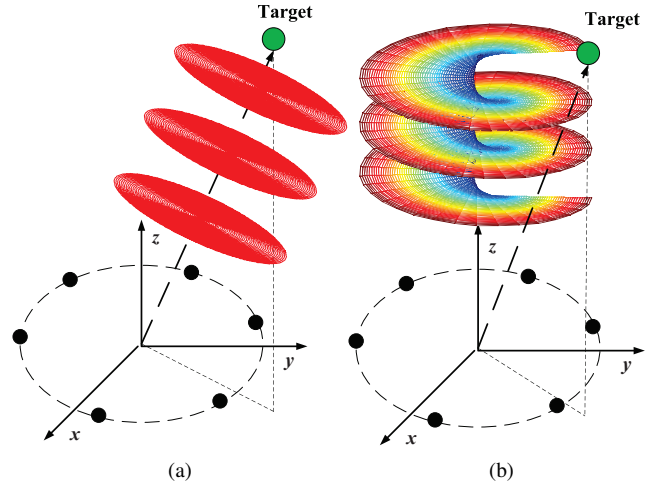


Fig. 1. Radar illuminate a target using (a) the traditional beam with planar wave (b) the twisted OAM beam with helical wavefront.

direction, the OAM-based radar employed twisted beams carrying different OAM modes to illuminate a target. This scenario provided a new perspective to estimate azimuthal information of targets without any relative moves or beam scanning as the traditional way required. Later, the detection model was further extended with Multiple Input Multiple Output (MIMO) and Multiple Input Single Output (MISO) schemes in [15]. Due to intrinsic drawbacks of the model, both schemes suffered from ambiguous problems, which require prior information involved as a solution. Under these two schemes, targets were usually not illuminated by main lobes of twisted beams, leading a significant energy loss of echo signals. To overcome this problem, several uniform concentric circular arrays (UCCAs) were deployed to enhance the energy of received signals in [16], with each ring producing a particular OAM mode and ensuring all main lobes were pointed at the same direction. This scenario benefited the detection for targets within main lobes in the noisy environment. Nevertheless, the low-resolution estimation method FFT were not capable to identify targets that within main lobes but with a narrow azimuth gap. Additionally, the performance of detection for targets not illuminated by the main lobes were not analyzed.

Based on the scenario in [16], this paper reconstructs the model for detecting targets within the main lobes for the super-resolution by using the MUSIC algorithm [17]. Furthermore, the estimation performance of targets being out of main lobes is further analyzed.

Mingtuan Lin, Peiguo Liu and Jibin Liu are with College of Electronic Science and Engineering, National University of Defense Technology, Changsha, 410073, China. (e-mail: mingtuan.lin@qmul.ac.uk; pg731@126.com; liujibin@nudt.edu.cn).

Mingtuan Lin and Yue Gao are with Queen Mary University of London, School of Electronic Engineering and Computer Science, London E1 4NS, UK. (email: yue.gao@qmul.ac.uk)

II. CURRENT OAM-BASED DETECTION MODELS

The MIMO and MISO schemes of OAM-based Radar techniques were investigated in [15]. For the MIMO scheme, the output summates the echo signals of all elements with the designed weights and a normalized real-time echo signal output of M targets can be extended and expressed as:

$$E(\alpha, t) = \sum_{m=1}^M \sigma_m \frac{e^{j2kr_m}}{r_m^2} e^{j2\alpha\varphi_m} J_\alpha^2(ka \sin \theta_m) s(t) + n(\alpha, t) \quad (1)$$

where α is the OAM mode, k is the wave number, J_α is the α th Bessel function, a is the radius of circular array, $s(t)$ is the transmitted signal, $n(\alpha, t)$ is the real time noise for OAM mode α , and $r_m, \theta_m, \varphi_m, \sigma_m$ refer to the distance, elevation, azimuth angle and the radar cross section (RCS) of m th target. For the MISO scheme, multiple antennas are employed at the transmitter to generate the twisted beams, while only one element is installed in the original point to receive the echo signals. The normalized echo signals is given by:

$$E(\alpha, t) = \sum_{m=1}^M \sigma_m \frac{e^{j2kr_m}}{r_m^2} e^{j\alpha\varphi_m} J_\alpha(ka \sin \theta_m) s(t) + n(\alpha, t) \quad (2)$$

By observing (1) and (2), a similar Fourier transform relation lies in α and φ regimes, which leads to the derivation of FFT [14]–[16] to make an estimation of the azimuth angles of targets. Both MISO and MIMO schemes can not ensure that targets are illuminated by main lobes of different OAM modes, which makes it vulnerable to the background noise.

N UCCAs with formulated apertures $a_i, i \in [1, N]$ as shown in Fig.2 were proposed to engender N OAM modes in [16] to tackle the above problem. In this scenario, larger aperture arrays in outer rings are used to generate higher modes twisted beams while inner rings create lower modes twisted beams, to make sure that targets can be illuminated by main lobes of each mode.

The normalized received echo signal using the UCCAs under the MIMO scheme can be written as:

$$E(\alpha, t) = \sum_{m=1}^M \frac{\sigma_m}{r_m^2} J_\alpha^2[ka(\alpha) \sin \theta_m] e^{j2\alpha\varphi_m} e^{j2kr_m} s(t) + n(\alpha, t) \quad (3)$$

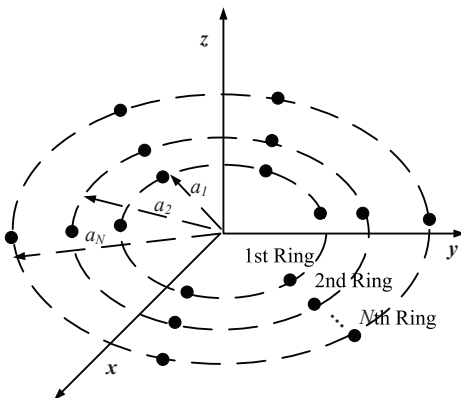


Fig. 2. Uniform concentric circular arrays.

where $a(\alpha) = \frac{1.02\alpha + 1.874}{k \sin \theta_0}$ refers to radius of the UCCA to create α mode with main lobe pointing at elevation angle θ_0 . Similar conclusions can be obtained for the MISO scheme.

III. PROPOSED ESTIMATION BASED ON THE MUSIC ALGORITHM

Despite the detection technique using the UCCAs could enhance the echo signal for targets within main lobes, the low-resolution estimation method FFT limits its application for detecting targets with narrow azimuth angle gaps. For targets within main lobes, this section rebuilds the model to achieve the super-resolution by using the MUSIC algorithm. It is assumed that the prior information of target number M is known.

A. MIMO scheme

According to (3), despite that main lobes of all OAM modes are pointing at θ_0 , there still exist echo energy difference for different modes. The energy differences can be eliminated by adjusting the array feeding gain $b(\alpha)$ for each mode, then the received echo signal is:

$$E(\alpha, t) = \sum_{m=1}^M \frac{\sigma_m}{r_m^2} b(\alpha) J_\alpha^2[ka(\alpha) \sin \theta_m] e^{j2\alpha\varphi_m} e^{j2kr_m} s(t) + n(\alpha, t) \quad (4)$$

Since targets are within main lobes, $\theta_m = \theta_0$. By designing the feeding gain of arrays for each mode

$$b(\alpha) = \frac{c}{J_\alpha^2[ka(\alpha) \sin \theta_0]} \quad (5)$$

thus (4) can be reformed as:

$$E(\alpha, t) = \sum_{m=1}^M e^{j2\alpha\varphi_m} c \frac{\sigma_m}{r_m^2} e^{j2kr_m} s(t) + n(\alpha, t) \quad (6)$$

where c is a constant. $E(\alpha, t)$ involves the data in terms of the α regime and t regime. By observing $e^{j2\alpha\varphi_m}$, φ_m in α regime can be understood as the angular frequency in time domain. Therefore, the estimation of φ_m in α domain is similar to estimate the angular frequency in time domain. Assume f_α is the sample rate in α regime, then according to the Nyquist sampling theory, to estimate φ_m without aliasing,

$$f_\alpha \geq 2f_{\max} = 2 \frac{w_{\max}}{2\pi}, w_{\max} \in [-2\pi, 2\pi] \quad (7)$$

where f_{\max} and w_{\max} indicates the max frequency and angular frequency in α regime, hence $f_\alpha \geq 2$. The echo signals under different OAM modes are not sampled simultaneously, which isn't applicable for the MUSIC algorithm. Fortunately, the time slot of the adjoint OAM modes is known, which could be calibrated to achieve the equivalent simultaneously sampling performance by delaying the corresponding time slot of $s(t)$ for specific OAM mode. Consider the calibrated real time echo

signals under N OAM modes, then the echo signal vector can be gained as:

$$\mathbf{E} = \begin{bmatrix} E(\alpha_1, t) \\ \vdots \\ E(\alpha_N, t) \end{bmatrix} = \mathbf{A}\mathbf{S} + \mathbf{n} = \begin{bmatrix} e^{j\alpha_1 2\varphi_1} \dots e^{j\alpha_1 2\varphi_M} \\ \vdots \\ e^{j\alpha_N 2\varphi_1} \dots e^{j\alpha_N 2\varphi_M} \end{bmatrix} \begin{bmatrix} \frac{c\sigma_2 e^{j2kr_1} s(t)}{r_1^2} \\ \vdots \\ \frac{c\sigma_M e^{j2kr_M} s(t)}{r_M^2} \end{bmatrix} + \begin{bmatrix} n(\alpha_1, t) \\ \vdots \\ n(\alpha_N, t) \end{bmatrix} \quad (8)$$

where $\mathbf{A} \in C^{N \times M}$ is the steering vector in α regime, $\mathbf{S} = [c\sigma_1 \frac{e^{j2kr_1}}{r_1^2} s(t), \dots, c\sigma_M \frac{e^{j2kr_M}}{r_M^2} s(t)]^T \in C^{M \times L}$ refer to echo signals of targets, L is the real time sample length of echo signals in the time domain. From (8), it can be observed that the steering vector \mathbf{A} is only related to the OAM mode α and φ , independent of the array shapes. For the direction of arrival (DOA) estimation, the steering vector depends on the space sampling method of the antenna i.e. the array shapes, while for the proposed model using the UCCAs to estimate the azimuth angles the steering vector is determined by the sampling method in α regime such as the uniform or sparse sampling. Under this proposed model, one OAM mode resembles one antenna in traditional DOA estimation model.

For presenting Gaussian noise, the covariance matrix of the echo signals under different OAM modes can be acquired by:

$$\mathbf{R}_E = \mathbf{A}\mathbf{R}_S\mathbf{A}^H + \rho_n\mathbf{I} \quad (9)$$

where ρ_n is the noise power. Similar to DOA estimation, columns of \mathbf{A} are independent, however the echo signals of multiple targets are fully coherent, falling to meet the uncorrelated condition for the MUSIC algorithm. Obviously, $\text{rank}(\mathbf{R}_S) = 1$, which means the leak from the signal subspace to the noise subspace and thus contaminate the orthogonality and deteriorate the performance of MUSIC. For traditional DOA estimation, spatial smoothing technique is utilized to tackle the coherent problem, which is only applicable for a uniform linear array (ULA), i.e. uniform space sampling array. Regarding to the proposed OAM-based radar model, the uniform linear OAM mode sampling in α regime is similar to the case of ULA for conventional DOA estimation. Therefore, the spatial smoothing is applicable to solve the coherent problem of the proposed model with uniform sampling. With appropriate reforms, other methods used in DOA estimation such as matrix decomposition can also solve the coherent problem in the proposed model. The spatial front smoothing technique is chose in this paper to conquer the coherent problem.

According to the smoothing theory [18], divide N OAM sample modes in α domain to p mixed subsamples blocks as shown in Fig.3. Each block has h modes, so $N = p + h - 1$. Subsequently, calculate the modified covariance matrix as follows:

$$\mathbf{R}^f = \frac{1}{p} \sum_{i=1}^p \mathbf{R}_i \quad \mathbf{R}^f \in C^{h \times h} \quad (10)$$

where \mathbf{R}_i is the covariance matrix of i th sub-block \mathbf{E}_i . To achieve the full rank of signal space, the number of blocks should meet $p \geq M$.

The whole procedure of the spatial smoothing MUSIC algorithm to estimate the azimuth angles is listed as follows:

- 1) Obtain p original covariance matrix \mathbf{R}_i ($i=1, 2, \dots, p$);
- 2) Gain \mathbf{R}^f based on (10).
- 3) Make engine value decomposition of \mathbf{R}^f .
- 4) Calculate the azimuth spectrum

$$P(\varphi) = \frac{1}{\mathbf{a}^H(\varphi)\mathbf{V}_n\mathbf{V}_n^H\mathbf{a}(\varphi)} \quad (11)$$

where \mathbf{V}_n is the noise subspace vectors obtained from the engine value decomposition of \mathbf{R}^f , $\mathbf{a}(\varphi) = [e^{j2\alpha_1\varphi}, \dots, e^{j2\alpha_N\varphi}]^T$ is the search steering vector.

B. MISO scheme

Similar conclusions can be retained for MISO scheme, but with several differences as follows:

- 1) To avoid aliasing, the minimum sample rate of MISO scheme is half that of MIMO scheme.
- 2) The resolution ability of MIMO scheme is double that of MISO scheme, with $\delta\varphi \propto \frac{1}{2\alpha}$ for MIMO scheme while $\delta\varphi \propto \frac{1}{\alpha}$ for MISO scheme.
- 3) The searching steering vector is $\mathbf{a}(\varphi) = [e^{j\alpha_1\varphi}, \dots, e^{j\alpha_N\varphi}]^T$.

IV. ANALYSIS FOR TARGETS OUT OF MAIN LOBES

The targets detection within designed main lobes is described in Section III, however for those objectives out of main lobes, $b(\alpha)J_\alpha^2[ka(\alpha)\sin\theta]$ or $b(\alpha)J_\alpha[ka(\alpha)\sin\theta]$ is not a constant for all modes. Would the proposed MUSIC algorithm estimate azimuthal information accurately? There is no doubt that for a windowing real-time signal with different frequencies MUSIC can calculate the spectrum successfully. Similarly, $b(\alpha)J_\alpha^2[ka(\alpha)\sin\theta]$ and $b(\alpha)J_\alpha[ka(\alpha)\sin\theta]$ can be regarded as a window for $e^{j2\alpha\varphi}$ and $e^{j\alpha\varphi}$ specifically. Consequently the MUSIC algorithm can gain a satisfactory estimation as predicted. But the influence caused by the window should be analyzed. Since the influence for MIMO and MISO schemes are similar, to avoid the repeated discussion, the following analyses are made under the MIMO scheme.

According to (3) and (4), the influence of estimation brought by the square Bessel function or its reformation can be seen as the influence of the point spread function (PSF) of the windowing. Here we consider the azimuth profile of PSF as

$$F(\varphi) = \int b(\alpha)J_\alpha^2(ka(\alpha)\sin\theta)e^{-j\alpha\varphi} d\alpha \quad (12)$$

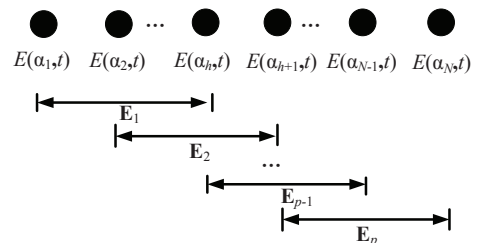


Fig. 3. Front-spatial smoothing in α regime.

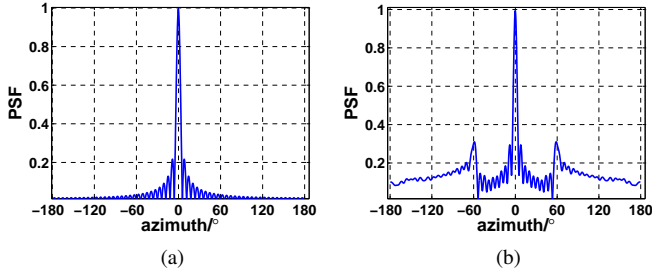


Fig. 4. Azimuth profile of PSF using the same UCCA configuration with main lobes aimed at 14° to illuminate targets with elevation (a) $\theta = 14^\circ$ (b) $\theta = 34^\circ$.

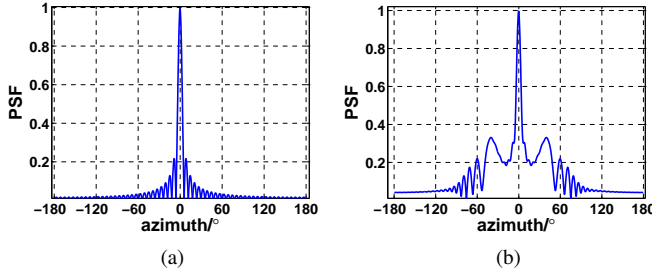


Fig. 5. Azimuth profile of PSF of the same target with $\theta = 14^\circ$ using (a) UCCA with $\theta_0 = 14^\circ$ (b) UCA with a radius equal to the outer ring of UCCA.

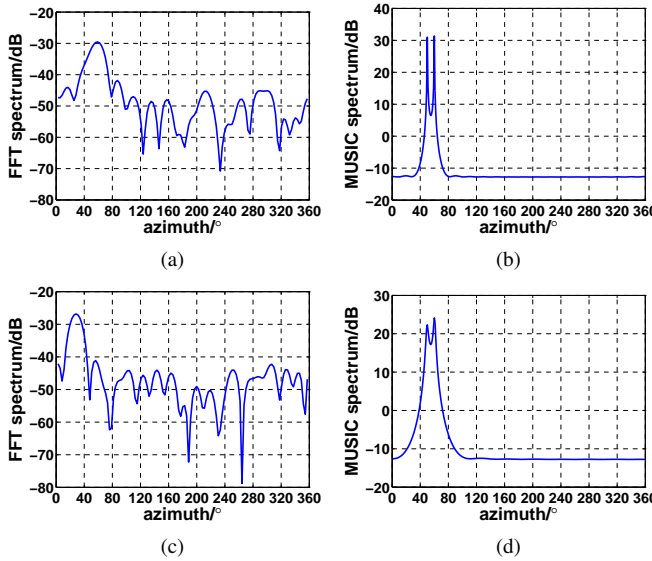


Fig. 6. Azimuth angle estimation spectrum under MIMO scheme: (a) and (b); MISO scheme: (c) and (d). (a) and (c) use the FFT method, while (b) and (d) utilize the MUSIC algorithm. Two targets at 782.4λ and 689.3λ with the same elevation angle 14° but different azimuth angles 50° and 60° are under illumination of main lobes of the UCCAs with configuration $N=60$, $f_\alpha = 2$, $L=1024$ at a SNR=10 dB environment.

According to signal processing theory, the multiplication relation in α regime indicates the convolution in φ field. By analyzing the profile of PSFs, the estimation performance of targets out of main lobes can be evaluated. Fig.4 compares

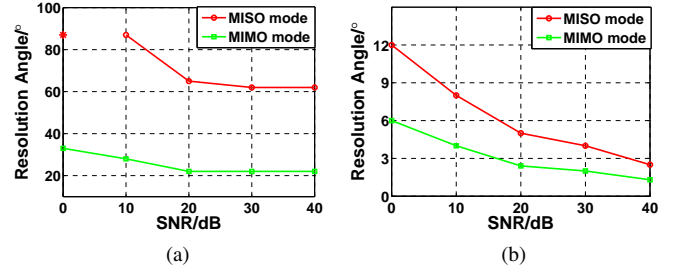


Fig. 7. Resolution angle against SNR using (a) FFT, (b) MUSIC. (* in (a) denotes no resolution ability for two targets).

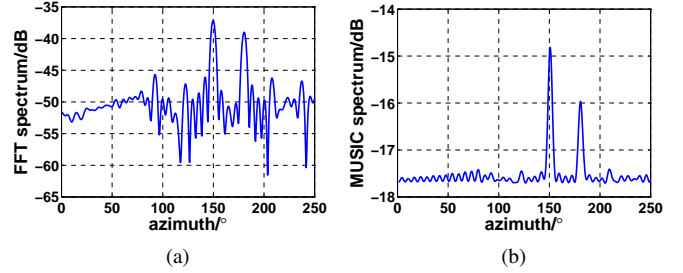


Fig. 8. Azimuthal estimation for targets out of main lobes using (a) FFT, (b) MUSIC. Directions of two targets are $(34^\circ, 150^\circ)$ and $(34^\circ, 180^\circ)$.

patterns of PSFs for targets with $\theta = 14^\circ$ and $\theta = 34^\circ$ specifically, using the same UCAA configuration with main lobes pointing at $\theta_0 = 14^\circ$. It can be observed for target not illuminated by main lobes, there are two high side lobes as shown in Fig.4 (b), while no side lobes in Fig.4 (a) appear for the target within main lobes. Those side lobes will introduce pseudo estimations into the azimuth spectrum, leading ambiguity problems for target detection. Influences caused by different array configurations to estimation can be also observed by figures of different PSFs as shown in Fig.5. Comparing Fig.4 and Fig.5, it can be implied that azimuthal estimation based on the UCCAs for targets out of main lobes will suffer the same ambiguity problem as a UCA configuration presented in [16].

V. SIMULATION

Simulations are presented to compare performances of the existing FFT method and the proposed MUSIC algorithm. Fig.6 illustrates comparisons of estimation performance between MIMO and MISO scheme, and between MUSIC and FFT method for targets within the main lobes. It can be observed that MUSIC has distinct higher resolution ability than that of FFT method for both schemes while MIMO scheme has a resolution advantage over that of MISO scheme. Specifically, the curve in Fig.7 gives the detailed information about the resolution of two schemes with two methods. Almost double resolution ability of MIMO scheme compared to MISO scheme can be viewed in Fig.7. By comparing Fig.7 (a) and (b), the super-resolution capacity of MUSIC for detection of targets within main lobes was apparently observed.

Using UCCA configuration as Fig.4 to illuminate two targets out of main lobes, four large ambiguous peaks appear in the spectrum of FFT in Fig.8 (a), in accordance with the side lobes of PSF in Fig.4. Side lobes in Fig.8 (b) also arise in MUSIC method but with great suppressions, which can be almost ignored. By comparing Fig.8 (a) and (b), it can be found that MUSIC has no great resolution advantage over FFT but instead is more robust than FFT with less ambiguity influence.

Overall, the proposed MUSIC algorithm improves the estimation performance of OAM-based radar detection using UCCA.

VI. CONCLUSIONS

For the OAM-based radar using the UCCAs, this paper addressed the MUSIC algorithm to improve the targets detection performance. Compared to the traditional FFT method, the proposed MUSIC shows the high-resolution capacity for the targets detecting within the main lobes, and good robustness for the targets detecting out of the main lobes. Benefiting from the high-resolution ability, the same performance as the FFT can be achieved by fewer number of OAM modes using MUSIC method and thus can reduce the design complexity and cost of the hardware. The proposed model was built with the ideal propagation loss, however the gain loss for each OAM mode of the real system could be complex and would introduce the deviation. Further work could be done about the calibration technique with the measured propagation loss difference of each OAM mode to reduce the estimation error.

REFERENCES

- [1] J. P. Torres and L. Torner, *Twisted photons: applications of light with orbital angular momentum*. John Wiley and Sons, 2011.
- [2] A. M. Yao and M. J. Padgett, "Orbital angular momentum: origins, behavior and applications," *Advances in Optics and Photonics*, vol. 3, no. 2, pp. 161–204, 2011.
- [3] B. Thid, H. Then, J. Sjolholm, K. Palmer, J. Bergman, T. Carozzi, Y. N. Istomin, N. Ibragimov, and R. Khamitova, "Utilization of photon orbital angular momentum in the low-frequency radio domain," *Phys. Rev. Lett.*, vol. 99, no. 8, p. 087701, 2007.
- [4] M. Barbuto, F. Trotta, F. Bilotti, and A. Toscano, "Circular polarized patch antenna generating orbital angular momentum," *Prog. Electromagn. Res.*, vol. 148, pp. 23–30, 2014.
- [5] A. Beniss, R. Niemiec, C. Brousseau, K. Mahdjoubi, and O. Emile, "Flat plate for oam generation in the millimeter band," in *EuCAP2013-European Conference on Antennas and Propagation*, 2013, Conference Proceedings, p. 1.
- [6] L. Cheng, W. Hong, and Z.-C. Hao, "Generation of electromagnetic waves with arbitrary orbital angular momentum modes," *Sci. Rep.*, vol. 4, 2014.
- [7] D. K. Nguyen, O. Pascal, J. Sokoloff, A. Chabory, B. Palacin, and N. Capet, "Antenna gain and link budget for waves carrying orbital angular momentum," *Radi. Sci.*, vol. 50, no. 11, pp. 1165–1175, 2015.
- [8] S. M. Mohammadi, L. K. Daldorff, J. E. Bergman, R. L. Karlsson, B. Thid, K. Forozesh, T. D. Carozzi, and B. Isham, "Orbital angular momentum in radio system study," *IEEE Trans. Antennas Propag.*, vol. 58, no. 2, pp. 565–572, 2010.
- [9] A. Tennant and B. Allen, "Generation of oam radio waves using circular time-switched array antenna," *Electron. Lett.*, vol. 48, no. 21, pp. 1365–1366, 2012.
- [10] O. Edfors and A. J. Johansson, "Is orbital angular momentum (oam) based radio communication an unexploited area?" *IEEE Trans. Antennas Propag.*, vol. 60, no. 2, pp. 1126–1131, 2012.
- [11] F. Tamburini, E. Mari, A. Sponselli, B. Thid, A. Bianchini, and F. Romanato, "Encoding many channels on the same frequency through radio vorticity: first experimental test," *New Journal of Physics*, vol. 14, no. 3, p. 033001, 2012.
- [12] X. Hui, S. Zheng, Y. Chen, Y. Hu, X. Jin, H. Chi, and X. Zhang, "Multiplexed millimeter wave communication with dual orbital angular momentum (oam) mode antennas," *Sci. Rep.*, vol. 5, 2015.
- [13] Y. Yan, G. Xie, M. P. Lavery, H. Huang, N. Ahmed, C. Bao, Y. Ren, Y. Cao, L. Li, and Z. Zhao, "High-capacity millimetre-wave communications with orbital angular momentum multiplexing," *Nat. Commun.*, vol. 5, 2014.
- [14] G. Guo, W. Hu, and X. Du, "Electromagnetic vortex based radar target imaging," (*in Chinese*) *J. Nat. Univ. Defense Technol.*, vol. 35, no. 6, p. 6, 2013.
- [15] K. Liu, Y. Cheng, Z. Yang, H. Wang, Y. Qin, and X. Li, "Orbital-angular-momentum-based electromagnetic vortex imaging," *IEEE Antennas Wireless Propag. Lett.*, vol. 14, pp. 711–714, 2015.
- [16] T. Yuan, H. Wang, Y. Qin, and Y. Cheng, "Electromagnetic vortex imaging using uniform concentric circular arrays," *IEEE Antennas Wireless Propag. Lett.*, 2015.
- [17] R. O. Schmidt, "Multiple emitter location and signal parameter estimation," *IEEE Trans. Antennas Propag.*, vol. 34, no. 3, pp. 276–280, 1986.
- [18] S. U. Pillai and B. H. Kwon, "Forward/backward spatial smoothing techniques for coherent signal identification," *IEEE Trans. Acoust., Speech, Signal Process.*, vol. 37, no. 1, pp. 8–15, 1989.